Cardiac tumour necrosis factor receptor-associated factor 7 mediates the ubiquitination of apoptosis signal-regulating kinase 1 and aggravates cardiac hypertrophy

Yan Che[1,2†], Yu-Ting Liu[1,2†], Zhao-Peng Wang[1,2,3], Yi-Zhou Feng[1,2], Hong-Xia Xia[1,2], Yuan Yuan[1,2], Heng Zhou[1,2], Hong-Liang Qiu[1,2], Man-Li Hu[4], Sha-Sha Wang[1,2], and Qi-Zhu Tang [ID] [1,2]*

[1]Department of Cardiology, Renmin Hospital of Wuhan University, Jiefang Road 238, Wuhan 430060, PR China; [2]Hubei Key Laboratory of Metabolic and Chronic Diseases, Wuhan University, Jiefang Road 238, Wuhan 430060, PR China; [3]Department of Cardiology, Taikang Tongji (Wuhan) Hospital, Wuhan 420060, PR China; and [4]Gannan Medical University, Ganzhou 341000, PR China

|	
Aims	Cardiac remodelling is a common pathophysiological process in the development of various cardiovascular diseases, but there is still a lack of effective interventions. Tumour necrosis receptor-associated factor 7 (TRAF7) belongs to the tumour necrosis factor receptor-associated factor family and plays an important role in biological processes. Previous studies have shown that TRAF7 mutations lead to congenital defects and malformations of the heart. However, the molecular mechanisms of TRAF7 in the underlying pathogenesis of pathological cardiac hypertrophy remain unknown. We aim to study the molecular mechanisms and effects of TRAF7 in cardiac remodelling and whether it has the potential to become a therapeutic target for cardiac remodelling.
Methods and results	The pressure overload–induced cardiac hypertrophy model in mice was established via transverse aortic constriction (TAC) surgery, and cardiomyocytes were treated with phenylephrine (PE) to induce hypertrophic phenotype. Levels of cardiac dysfunction and remodelling were measured with echocardiography and tissue or cell staining. RNA sequencing, western blot, qRT–PCR, co-immunoprecipitation, and *in vivo* ubiquitination assays were used to explore the molecular mechanisms. The results showed that the expression of TRAF7 increased gradually during the development of hypertrophy. Accordingly, TRAF7 significantly exacerbated the PE-induced enlargement of primary neonatal Sprague-Dawley rat cardiomyocytes, whereas TRAF7 knockdown alleviated the hypertrophic phenotype in primary cardiomyocytes. Cardiac-specific overexpression of TRAF7 accelerated hypertrophic phenotype in mice and cardiac-specific *Traf7* conditional knockout mice improved hypertrophic phenotype induced by TAC. Mechanistically, TRAF7 directly interacted with apoptosis signal-regulating kinase-1 (ASK1) and promoted ASK1 phosphorylation by mediating the K63-linked ubiquitination of ASK1 in response to PE stimulation, which then promoted ASK1 activation and downstream signalling during cardiac hypertrophy. Notably, the pro-hypertrophic effect of TRAF7 was largely blocked by GS4997 *in vitro* and cardiac-specific *Ask1* conditional knockout *in vivo*.
Conclusion	In summary, we identified TRAF7 as an essential regulator during cardiac hypertrophy, and modulation of the regulatory axis between TRAF7 and ASK1 could be a novel therapeutic strategy to prevent this pathological process.

---

* Corresponding author. Tel: +8627 8073385; fax: +8627 88042292, E-mail: qztang@whu.edu.cn
† Yan Che and Yu-Ting Liu are co-first authors and contributed equally.

Graphical Abstract
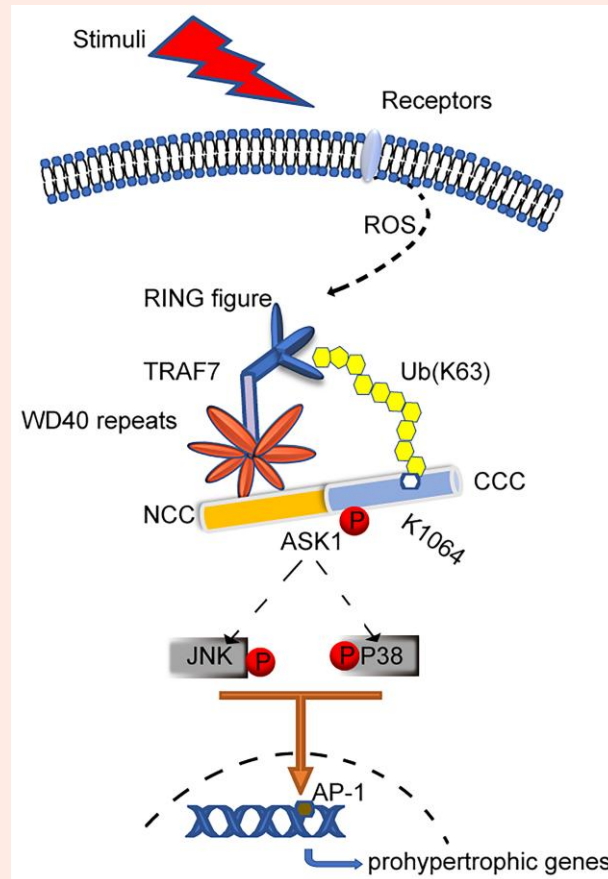
A schematic diagram of the molecular mechanisms underlying tumour necrosis receptor-associated factor 7 (TRAF7)-regulated cardiac hypertrophy. Under hypertrophic stimulation, reactive oxygen speeces (ROS)-triggered TRAF7 expressing binds to the apoptosis signal-regulating kinase-1 (ASK1) through its WD40 repeats domain and applies the ring domain to promote the ubiquitination of lys1064 in ASK1 via the K63 ubiquitin chain, thereby promoting ASK1 phosphorylation and then activating JNK/p38 axis in cardiomyocytes.

1. Introduction

Cardiac hypertrophy is a maladaptive change in cardiomyocytes in response to adverse stimulation that occurs in the process of many cardiovascular diseases such as hypertension, myocardial infarction/ischaemic disease, and congenital heart disease and eventually develops into severe arrhythmia and heart failure (HF).[1,2] Numerous studies have confirmed the role of the mitogen-activated protein kinase (MAPK) in the progression of cardiac hypertrophy, in which P38MAPK and JNK promote the development of cardiac hypertrophy by regulating inflammation, oxidative stress, and apoptosis.[3,4] Therefore, inhibiting the MAPK signalling pathway may effectively improve or delay the procession of cardiac hypertrophy.

As an important component of tumour necrosis factor (TNF) superfamily signal transduction, TNF receptor-associated factors (TRAFs) are mainly involved in the activation of the MAPK and NF-κB signalling pathways and play important roles in the regulation of inflammation, proliferation, differentiation, and apoptosis.[5] To date, seven TRAFs have been identified in mammals. It has been reported that some of the TRAFs play a role in cardiac hypertrophy. Transgenic mice overexpressing TRAF2 driven by major histocompatibility complex (MHC) promoter showed the symptoms of progressive cardiac hypertrophy with increased myocardial fibrosis.[6]

Overexpressing TRAF3 or TRAF6 in the heart developed exaggerated cardiac hypertrophy in response to pressure overload.[7,8] *Traf5* knockout mice showed the substantially aggravated cardiac hypertrophy compared with fibrosis.[9] TRAF1–6 each have a conserved amino acid structure at the C terminus called the TRAF domain.[10] TRAF1–6 participate in the activation of MAPK through the binding of the classic TRAF domain and signalling molecules. In addition, TRAF2, TRAF5, and TRAF6 can also enhance the ubiquitination and autophosphorylation of apoptosis signal-regulating kinase-1 (ASK1), a member of the mitogen-activated protein kinase kinase kinase (MAP3K) family that can directly activate JNK and P38MAPK by binding its ring domain.[11] Similar to other TRAFs, TRAF7 has a ring finger domain and several adjacent zinc finger domains at the N terminus. However, TRAF7 does not contain the TRAF domain structure, and its C terminus has seven specific WD40 repeats,[12] which are associated with downstream molecular signal transduction. A previous study showed that the activation of MAPK by TRAF7 depends on its seven C-terminal WD40 repeats, which can bind to MEKK3 to activate P38MAPK and JNK in response to tumour necrosis factor alpha (TNF-α) stimulation in tumour cells.[13]

Several studies have confirmed that congenital defects and malformations of the heart, such as ventricular septal defects, patent ductus

arteriosus, and coarctation of the aorta, have been observed in patients with TRAF7 mutations.[14,15] However, the role of TRAF7 in the cardiovascular system remains largely unknown. In the present study, we found that the expression of TRAF7 was significantly increased in hypertrophic cardiomyopathy induced by pressure overload in mice, indicating that TRAF7 may affect in this process. We hypothesized that TRAF7 exacerbated cardiac hypertrophy by inducing the phosphorylation of ASK1 and subsequently activating the MAPK signalling cascade. In this study, we used adeno-associated virus (AAV9)-mediated overexpression of TRAF7 mice, cardiac-specific *Traf7* conditional knockout mice, cardiac-specific *Ask1* conditional knockout mice, and TRAF7-deficient or overexpressed neonatal rat ventricular myocytes to investigate the role of TRAF7 in pressure overload–induced cardiac hypertrophy.

2. Methods

2.1 Reagents

Phenylephrine (PE, P6126) was purchased from Sigma-Aldrich (Missouri, USA). The BCA Protein Assay Kit (23225) was procured from Thermo Fisher Scientific (Massachusetts, USA). The DMEM/F12 medium (C11330500BT) and foetal calf serum (FCS, 22011-8612) were obtained from Gibco (California, USA) and Tianhang Biotechnology Co., Ltd (Hangzhou, China), respectively.

GS-4997 is a highly selective ASK1 inhibitor that competes with ATP in the ASK1 catalytic kinase domain.[16]

2.2 Experimental animals

Male C57BL/6 mice, 8 weeks old, were obtained from the Institute of Laboratory Animal Science, Chinese Academy of Medical Sciences (Beijing, China) and kept under constant environmental conditions with 12 h light/dark cycles and allowed free access to food and water. The investigation conformed to the Guide for the Care and Use of Laboratory Animals published by the US National Institutes of Health (NIH publication no. 85-23, revised 1996). The Institutional Animal Care and Use Committee of the Institute of Model Animals of Wuhan University and the Animal Care and Use Committee of Renmin Hospital of Wuhan University approved all animal protocols.

To further verify the role of TRAF7 *in vivo*, the mice were subjected to AAV9-*Traf7* or AAV9-GFP injection 4 weeks before TAC or sham operations to overexpression TRAF7. AAV9-*Traf7* and AAV9-GFP were constructed and generated by Vigene Biosciences (Shandong, China). Briefly, recombinant adeno-associated virus-9 (AAV9) harbouring full-length mouse TRAF7 gene with the cardiac troponin T (cTNT) promotor (AAV9-cTNT-*Traf7*) and control vectors (AAV9-cTNT-GFP) were prepared and delivered as described before.[17] Viral particles [1×10^{12} vector genomes per animal in a total of 100 µL phosphate buffered saline (PBS)] were administered to 4- to 5-week-old mice through tail injection.[18]

Besides, under the background of C57BL/6, the *Traf7* conditional knockout (*Traf7*-CKO) mice were generated. Briefly, sgRNA and the donor vector containing loxP were designed by using the CRISPR design tool (http://chopchop.cbu.uib.no/). The mixture of the Cas9 mRNA, sgRNA, and donor vector was microinjected into the single fertilized eggs of C57BL/6 by using the FemtoJet 5247 microinjection system. Genotyping was carried out on the DNA extracted from tail biopsies with the following primers: F: 5′-TGGGTCTCACACGGCATTCC-3′; R: 5′-CATCCAGCAGCCAATCATGG-3′. Mice carrying the recombinant allele (*Traf7*$^{fl/fl}$) were subsequently obtained via the generation of *Traf7*^{fl}.

Then, the *Traf7*$^{fl/fl}$ mice were crossed with Myh6-cre/Esr1 (Jackson Laboratory, 005650, Maine, USA) to generate *Traf7*$^{fl/fl}$/α-MHC-MerCreMer mice. To activate Cre recombinase, tamoxifen (25 mg/kg/d, Sigma-Aldrich, T5648, Missouri, USA) was administered to all experimental *Traf7*$^{fl/fl}$/α-MHC-MerCreMer mice via intraperitoneal injection for 5 consecutive days. *Traf7*^{fl} mice were also treated with equal doses of tamoxifen injection as the controls.

Ask1$^{fl/fl}$ mice were gifted from the Institute of Model Animal of Wuhan University (Wuhan, China), and *Ask1*-CKO mice were obtained after crossbreeding according to the above method.

2.3 Transverse aortic constriction and echocardiography

Pressure overload–induced cardiac hypertrophy model was established by transverse aortic constriction (TAC) surgery. In short, the mice were first anaesthetized with pentobarbital sodium (intraperitoneal injection, 80 mg/kg, Sigma-Aldrich, P3761) or isoflurane inhalation and kept on a heating pad to maintain the body temperature as close as 37°C. For isoflurane inhalation, the mice were connected to a ventilator and 4–5% were used for induction and 2–3% were used for maintenance of general anaesthesia throughout the TAC surgery and echocardiography. To expose aortic arch, a small incision was made after the animal was deeply anaesthetized. Then, a 7-silk suture was placed around the transverse aorta between the brachiocephalic and left carotid artery and ligated with a 26-gauge needle, which was then removed. Finally, the chest was sutured closed and the postoperative mice were kept in a 37°C incubator until recovery. The sham group was only induced by chest open and close without ligation.

The mice were subjected to echocardiography 4 weeks after TAC operation by using a MyLab 30CV ultrasound system (Maryland, USA) with a 10-MHz phased array transducer. Parameters of cardiac function as left ventricular end-systolic diameter (LVEDs) and left ventricular end-diastolic diameter (LVEDd) were measured from M-mode short-axis images at the level of the papillary muscles for a time period of more than five consecutive cardiac cycles. Left ventricular fraction shortening (FS) was assessed by B-mode long-axis images. The ejection fraction (EF) was calculated based on LVEDs and LVEDd. The mice were euthanized by performing cervical dislocation under deep anaesthesia caused by pentobarbital sodium (intraperitoneal injection, 80 mg/kg, Sigma-Aldrich, P3761, Missouri, USA) or 2.5% isoflurane inhalation. The heart tissue was fixed in 4% paraformaldehyde or frozen in liquid nitrogen for subsequent pathological and molecular analyses.

2.4 Cell culture and adenoviral infection

Neonatal Sprague-Dawley rat cardiomyocytes (NRCMs) and neonatal rat cardiac fibroblasts (NRCFs) were enzymatically isolated from 1- to 3-day-old Sprague-Dawley rat heart. Briefly, the rats were anaesthetized using isoflurane and sacrificed. Then, heart tissues were harvested and digested with PBS containing 0.03% trypsin and 0.4% collagenase Type II. NRCMs were seeded at a density of 2×10^6 cells per well in six-well culture plates. Both NRCMs and NRCFs were cultured in 10% foetal bovine serum (Gibco; Thermo Fisher Scientific Inc., Grand Island, NY, USA) and Dulbecco's modified Eagle's medium/F12 medium for 24 h before being used in the subsequent experiments. NRCMs were infected with adenovirus shRNA-control, shRNA-*Traf7*, Ad-Con, or Ad-*Traf7* [multiplicity of infection (MOI) = 50] for 12 h and keep culturing for 12 h, followed by the subsequent experiments.

2.5 Western immunoblotting

Protein samples from cells and tissues were lysed in buffer containing protease and phosphatase inhibitors before being separated by 8–10% sodium dodecyl sulphate–polyacrylamide gel electrophoresis (SDS–PAGE) and transferred to polyvinylidene difluoride (PVDF) membranes. After blocking, the membranes were incubated with primary antibodies at 4°C overnight. On the next day, after washing with PBS, the membranes were incubated with appropriate secondary antibodies for 1 h at room temperature before being washed three times with Tris Buffered Saline Tween. The blot signals were detected by using an enhanced chemiluminescence (ECL) detection system after incubating with ECL reagents (Bio-Rad 170-5061). Densitometric quantification was analysed with ChemiDoc XRS + System (Bio-Rad, California, USA). GAPDH or total protein levels were used as control in cell and tissue samples. The antibodies used in this study are listed in Supplementary material online, *Table S1*.

2.6 Quantitative real-time PCR

Total mRNA was isolated from the left ventricular tissues or cells using TRI reagent (Sigma, T9424) and was reverse-transcribed with Transcriptor HiScript III RT SuperMix for qPCR (+gDNA wiper) (Vazyme, R323-01). Then, by using a LightCycler480 system (Roche, Basel, Switzerland) and SYBR qPCR Master Mix (2×) (Vazyme, Q311-03, Nanjing, China), target mRNA expression levels were measured. The relative mRNA levels were normalized against GAPDH mRNA levels. The primer sequences used are provided in Supplementary material online, *Table S2*.

2.7 RNA-seq

Total RNA was extracted from NRCMs infected with Ad-con or Ad-Traf7 treated with PE for 24 h using TRIzol reagent. RNA library preparation was then prepared using MGIEasy RNA Library Prep Kit following the manufacturer's instructions. A gene expression analysis was performed by mRNA sequencing on a BGISEQ-500 (MGI Tech Co., Ltd, Shenzhen, China) with a single-end 50 bp module.

2.8 *In vivo* ubiquitination assays

Cells or heart tissues were lysed in 100 μL IP lysis buffer with 1% SDS and then were denatured via heating for 15 min at 95°C. The supernatants were diluted 10-fold with IP buffer. After sonication, the lysates were centrifuged at 12 000 rpm for 15 min at 4°C. The supernatants were subjected to immunoprecipitation with the indicated antibodies. After adding protein G agarose (11719416001; Roche), equal amounts of lysate were incubated with the indicated antibodies for 4 h at 4°C with gentle rotation. Subsequently, immunoprecipitates were washed three times with IP buffer. Proteins eluted from beads were used for western blots.

2.9 Immunofluorescence staining

To better position TRAF7, we double-strained with α-actinin and TRAF7 using paraffin sections of heart tissues. Briefly, the sections were antigen repaired and blocked as described above and then incubated with diluted primary antibody (TRAF7, Proteintech, 1:100 dilution; α-actinin, CST, 1:1000 dilution) at 4°C overnight. After washing the slices three times with PBS , the slides were incubated with an appropriate fluorescent secondary antibody (anti-rabbit IgG (H + L), CST, #4412, 1:1000 dilution, CoraLite594-conjugated Goat Anti-Mouse IgG(H + L), Proteintech, SA00013-3, 1:200 dilution) for 1 h. After washing three times with PBS, DAPI was used to label the nuclei. Finally, images were acquired by using a fluorescence microscope.

To evaluate the cell surface size, the NRCMs were assessed by immunofluorescent straining. Cardiomyocytes were treated with PE for 24 h after infection with corresponding adenovirus for 24 h. For straining, the NRCMs were first fixed with 4% formaldehyde for 15 min at room temperature and washed with PBS three times. Then, the cells were permeabilized with 0.2% Triton X-100 in PBS for 10 min at room temperature before being stained with primary antibody of α-actinin (Sigma, A78811, 1:100 dilution) at 37°C for 2 h. Finally, after washing three times with PBS, the cell slides were incubated with the appropriate fluorescent secondary antibody (goat anti-mouse IgG (H + L) secondary antibody, Invitrogen, A11029, 1:200 dilution). Images were obtained by using a confocal laser scanning microscope (TCS SP8, LEICA, Wetzlar, Germany). The quantitative digital image analysis system (Image-Pro Plus 6.0) was used to quantify the cell surface size.

For colocalization experiments, NRCMs were co-transfected with plasmids encoding HA-tagged ASK1 and Flag-tagged TRAF7 for 36 h. Then, the cells were double-stained as previous described with anti-Flag and anti-HA antibodies. After incubating with the corresponding fluorophore-conjugated secondary antibody, images were acquired by using a confocal microscope. Besides, heart tissues were double-stained with anti-TRAF7 (Proteintech, 11780-1-AP, 1:100 dilution) and anti-ASK1 (Proteintech, 67072-1-Ig, 1:100 dilution) antibodies as previous described, and images were obtained by using the confocal laser scanning microscope.

2.10 Cardiac morphology and histological analysis

Tissue sections were obtained as previous described, and haematoxylin–eosin (HE) staining was used to count cell surface area and picrosirius red (PSR) staining was used to count LV collagen volume. The quantification of cross-sectional area (CSA) of the cells and LV collagen volume were analysed with a quantitative digital analysis imaging system (Image-Pro Plus 6.0).

2.11 Immunoprecipitation assays

HEK293T cells were collected with ice-cold PBS after 24 h transfection and then lysed in ice-cold IP buffer (20 mM Tris–HCl pH 7.4, 150 mM NaCl, 1 mM EDTA, and 1% Triton X-100) containing protease inhibitor cocktail and phosphatase inhibitor PhosStop. After being treated by ultrasonic, the lysates were centrifuged at 12 000 rpm at 4°C for 10 min. Then, the supernatants were incubated with protein G Bestarose 4FF beads (Bestchrom, AA304307) and antibodies for 4 h. The beads were washed three times with ice-cold IP buffer. Finally, the beads were heated in loaded buffer at 95°C and analysed by western blot.

To better show the interaction between endogenous TRAF7 and ASK1, we performed co-immunoprecipitation (Co-IP) using cardiac tissue. Briefly, fresh left ventricular tissue was extensively lysed in immunoprecipitation buffer supplemented with protease/phosphatase inhibitors (Beyotime, P0013J). Subsequently, the heart tissue was fully broken in a grinder precooled at 4°C, lysed for 10 min, and centrifuged, and the supernatant containing total protein was collected. The total protein concentration was measured by using a BCA protein concentration measurement kit, and the quantified protein was used for Co-IP. The samples were incubated with specific primary antibodies or IgG at 4°C for 4 h by rotation. Afterwards, protein A/G agarose beads were added to the mixed samples and incubated at 4°C for 2 h by rotation. After incubation, the samples were washed three times with immunoprecipitation buffer and the protein mixture was boiled and analysed by western blot.

2.12 GST pulldown assay

In order to analyse the interaction between ASK1 and TRAF7, ASK1- and TRAF7-glutathione *S*-transferase (GST) fusion proteins were synthesized in *Escherichia coli* DH5α cells. Transformed bacteria were grown at 37°C until A_{600} up to 0.6 and then induced with isopropyl 1-thio-β-D-galactopyranoside at a concentration of 1 mM for 3 h. Cells were lysed with five freeze–thaw cycles and then treated with 1 min of sonication. After centrifugation, the soluble fraction combined with glutathione–Sepharose beads in an EconoPac chromatography column (Bio-Rad) overnight on a rotating wheel at 4°C. The beads were then washed twice with PBS and resuspended in lysis buffer with protease and phosphatase inhibitors. Flag-TRAF7 and Flag-ASK1 were purified from HEK294T cells expressing indicated protein using protein G agarose beads, Flag-tagged antibodies. The purified GST-HA-TRAF7 or GST-HA-ASK1 was incubated with glutathione–Sepharose 4B beads for 1 h before incubation with Flag-ASK1 or Flag-TRAF7 for 4 h at 4°C, respectively. After washing three times with GST buffer, samples were boiled for 5 min at 95°C, and supernatants were separated by SDS–PAGE and tested by western blotting.

2.13 Plasmids construction and adenoviral vectors

The PCR-amplified segments of full-length and truncated human ASK1 or TRAF7 were inserted into pcDNA5 vectors or pGEX-6p-GST vectors according to the following method.[19]

As for obtaining a series of variant ASK1 constructs with lysine mutated to arginine, first primers for mutation sites of ASK1 were designed, and after PCR and digesting by *Dpn*I, the enzymatic cleavage products were transformed using 100 μL JM109 receptive bacteria. Mutants of ASK1 plasmids were cultured by loading buffer with 100 μg/mL ampicillin and

obtained after being sequenced. The primer sequences used are provided in Supplementary material online, Table S3.

To generate adenoviral vectors for overexpressing *Traf7* and *Ask1* or its mutant, we utilized the shuttle plasmid pENTR-U6-CMV-flag-T2A along with the adenoviral expression system (V493-20; Invitrogen, CA, USA). The recombinant adenoviral vector was linearized using *PacI* and co-transfected into 293A cells using polyethyleneimine (PEI; 24765-1, Polysciences Inc., Warrington, PA, UK). After 1 week of culture, the cells were collected and purified by caesium chloride density gradient centrifugation.

2.14 Statistical analysis

All data were expressed as mean ± SD from three independent experiments and analysed using the appropriate statistical analysis methods. Student's two-tailed *t*-test was used to compare the mean values between two groups. One-way analysis of variance (ANOVA) was used to compare multiple groups of samples and then followed by the Bonferroni analysis for data meeting homogeneity or Tamhane's T2 analysis for data demonstrating heteroscedasticity. Statistical Package for the Social Sciences (SPSS) 21.0 software was used for all statistical analysis. *P* values < 0.05 were considered significant.

3. Results

3.1 TRAF7 expression is increased in experimental hypertrophic models

Western blot analysis showed that TRAF7 protein expression was significantly increased in a mouse cardiac hypertrophy model established by TAC, which was consistent with the levels of the prohormone atrial natriuretic peptide (ANP) (*Figure 1A* and *B*). Immunohistochemistry staining further confirmed that TRAF7 protein levels were increased after TAC (*Figure 1C*). Similarly, the protein levels of TRAF7 were up-regulated in PE- or angiotensin II (AngII)-induced NRCMs which occurred in parallel with the up-regulation of the foetal gene ANP (*Figure 1D*). The mRNA levels of TRAF7 were also up-regulated in PE-induced NRCMs and TAC-induced overload models in mice (see Supplementary material online, Figure S1A and B). However, the protein levels of TRAF7 were not significantly changed in PE- or AngII-induced NRCFs although the Collagen Type I Alpha 1 Chain (COL1A1) level increased markedly (*Figure 1E*). Furthermore, the majority of TRAF7 expression was detected in cardiomyocytes, where it could be colocalized with the marker protein of cardiomyocytes, α-actinin (*Figure 1F*). In addition, we assessed the protein and mRNA levels of TRAF7 and ANP at 3 days, 5 days, and 1 week after TAC, and our results showed that TRAF7 protein and mRNA expression were already up-regulated at 3 days after TAC, while ANP did not exhibit significant differences compared with the sham group. This indicates that the TRAF7 up-regulation occurs prior to hypertrophy and remodelling processes (see Supplementary material online, Figure S1C–E). Overall, these results suggest that increased TRAF7 expression in NRCMs may play a critical role in regulating cardiac hypertrophy and function.

As ROS is an important factor in stress overload and G-protein-coupled receptor agonist (PE/AngII)-induced cardiac remodelling signalling pathway and ROS is required for many TRAFs activation, we investigated whether ROS is the factor that causes an increase in TRAF7. In *in vitro* studies, we found that TRAF7 can be activated by ROS (see Supplementary material online, Figure S3A), and ROS scavenger *N*-acetyl-cysteine can inhibit TRAF7 expression in cell models induced by PE/AngII (see Supplementary material online, Figure S3B).

3.2 TRAF7 promotes cardiomyocyte hypertrophy *in vitro*

To determine whether TRAF7 regulates the development of cardiomyocyte hypertrophy, we generated cardiomyocytes with TRAF7 overexpression or down-regulation by infecting the cells with adenovirus or shRNA and inducing hypertrophy with PE. First, we confirmed TRAF7 overexpression and down-regulation by western blotting (*Figure 2A* and *B*, see Supplementary material online, Figure S2A and B). The immunofluorescence staining of α-actinin revealed a notable rise in the morphology area of cardiomyocytes in Ad-*Traf7*-infected NRCMs compared with control cells. Conversely, *Traf7* knockdown prevented PE-induced cardiac hypertrophy (*Figure 2C*). In parallel, Ad-*Traf7* exhibited a heightened level of ANP compared with the control group, signifying that TRAF7 overexpression fostered the expression of cardiac hypertrophic protein, whereas TRAF7 knockdown had inverse effects (*Figure 2F*). Furthermore, the overexpression of TRAF7 promoted the elevation of genes that participate in the stimulation of cardiac hypertrophy (e.g. *Anp*, *Bnp*, and *Myh7*) in response to PE treatment, whereas the reduction of TRAF7 expression curbed the expression of these hypertrophic genes (*Figure 2D* and *E*).

3.3 Cardiac-specific overexpression of TRAF7 accelerates cardiac remodelling

To better examine the phenotype associated with TRAF7 and pressure overload–induced cardiac hypertrophy, we used AAV vectors to deliver genes driven by the proximal promoter of cardiomyocyte-specific cTNT to overexpress TRAF7 in mouse hearts, and the schematic diagram of the animal experiment is shown in *Figure 3A*. A vector dose of 1×10^{12} led to TRAF7 eight–nine-fold overexpression at the protein level in the heart tissue (*Figure 3B*, see Supplementary material online, Figure S2C). At 2 weeks after injection, we performed TAC and evaluated cardiac function after 4 weeks. Consistent with the *in vitro* findings, overexpression of TRAF7 exacerbated TAC-induced cardiac hypertrophy. Compared with those of control AAV-GFP-injected mice after TAC, heart weight and the HW/BW, LW/BW, and HW/TL ratios were increased (*Figure 3C*). Moreover, TRAF7 markedly deteriorated left ventricular contractile function compared with that of control AAV-injected mice after TAC, as evidenced by the decreases in LVEDd, LVESd, EF%, and FS% (*Figure 3D*). HE staining showed a notable increase in the CSAs of myocytes in mice with cardiac TRAF7 overexpression compared with control AAV-GFP-injected mice at 4 weeks after TAC (*Figure 3E*). PSR straining showed that TAC-induced cardiac interstitial fibrosis and perivascular fibrosis were both worsened by TRAF7 overexpression (*Figure 3E*). Consistently, the mRNA levels of hypertrophic genes (e.g. *Anp*, *Bnp*, and *Myh7*) and cardiac fibrosis-related genes (e.g. *Col1a1*, *Col3a1*, and *Ctgf*) were significantly increased in the AAV9-*Traf7* group compared with the AAV9-GFP TAC group (*Figure 3F*). Overall, TRAF7 overexpression accelerates heart dysfunction, cardiac hypertrophy, and heart remodelling.

Then, we generated a knockout mouse model, *Traf7*-CKO mice, to assess the TRAF7 function *in vivo*. The efficiency of *Traf7*-CKO in the heart is demonstrated in *Figure 4A* and *B* by western blot. The outcomes of *Traf7* knockout are exactly opposite to those observed in TRAF7 overexpression (*Figure 4C–F*). As apoptosis plays a significant role in cardiac fibrosis, we assessed the apoptosis level in TRAF7 overexpression and *Traf7*-CKO mice. The results of both WB and TUNEL staining indicated that TRAF7 overexpression fosters apoptosis induced by stress overload, whereas *Traf7* knockout significantly diminishes apoptosis (see Supplementary material online, Figure S4A–C).

3.4 TRAF7 promotes cardiac hypertrophy via the MAPK signalling pathway

To investigate the involvement of cardiac *Traf7*-mediated changes in the regulation of cardiac hypertrophy, we performed RNA-seq analysis of PE-induced NRCMs infected with control or *Traf7* adenovirus. Hierarchical clustering showed that Traf7 was the main factor that influenced clustering (*Figure 5A*). Differentially expressed genes (DEGs) were identified via the volcano plot, which showed that 1571 genes were up-regulated, while 2198 genes were down-regulated by *Traf7* (*Figure 5B*). The results of gene set enrichment analysis (GSEA) of the cardiac
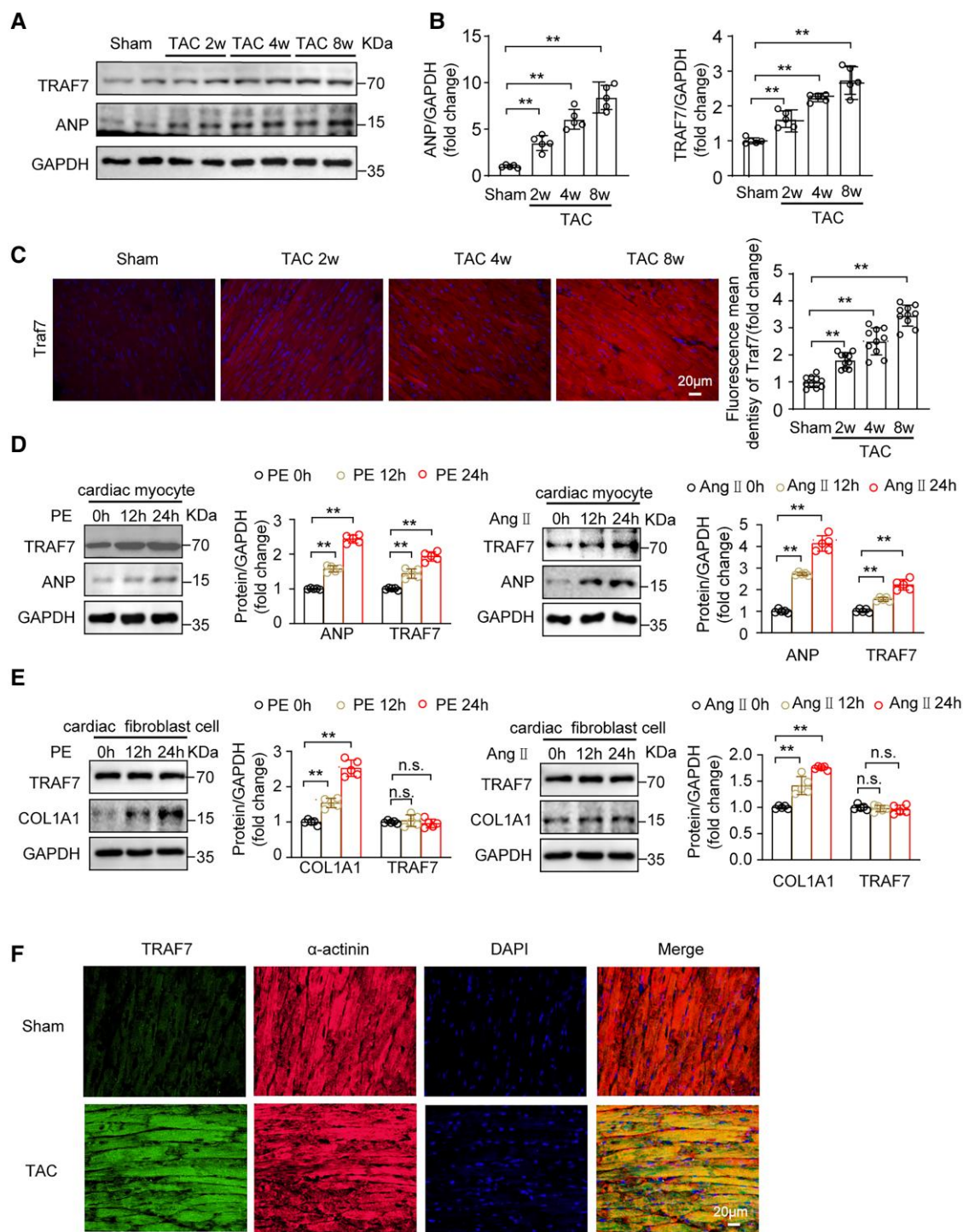
Figure 1 TRAF7 expression is increased in experimental hypertrophic models. (*A*) Representative western blots and (*B*) quantitative results of ANP and TRAF7 expression in cardiac left ventricle tissues from mice subjected to sham or TAC surgery for the different time periods (*n* = 5). GAPDH served as internal control. (*C*) Representative images and quantitative results showing immunofluorescence staining for TRAF7 of heart tissue sections from mice at sham or subjected to TAC surgery for the different time periods (*n* = 10). Scale bar: 20 μm. (*D*) TRAF7 and ANP expression in NRCMs treated with or without PE (50 μM) or AngII (1 μM) for 12 and 24 h compared with PBS-treated controls (*n* = 5). (*E*) Representative western blots and quantitative results of TRAF7 and COL1A1 expression in CFs treated with or without PE or AngII for 12 and 24 h compared with PBS-treated controls (*n* = 5). (*F*) Representative images of immunofluorescence staining for TRAF7 and α-actinin in mice heart tissues sections at 4 weeks after sham or subjected to TAC surgery. Nuclei were labelled with DAPI. Scale bar: 20 μm (*n* = 5). All data are shown as the mean ± SD. Significance analysed by one-way ANOVA with the Bonferroni analysis for data meeting homogeneity or Tamhane's T2 post hoc analysis. *P < 0.05, **P < 0.01.
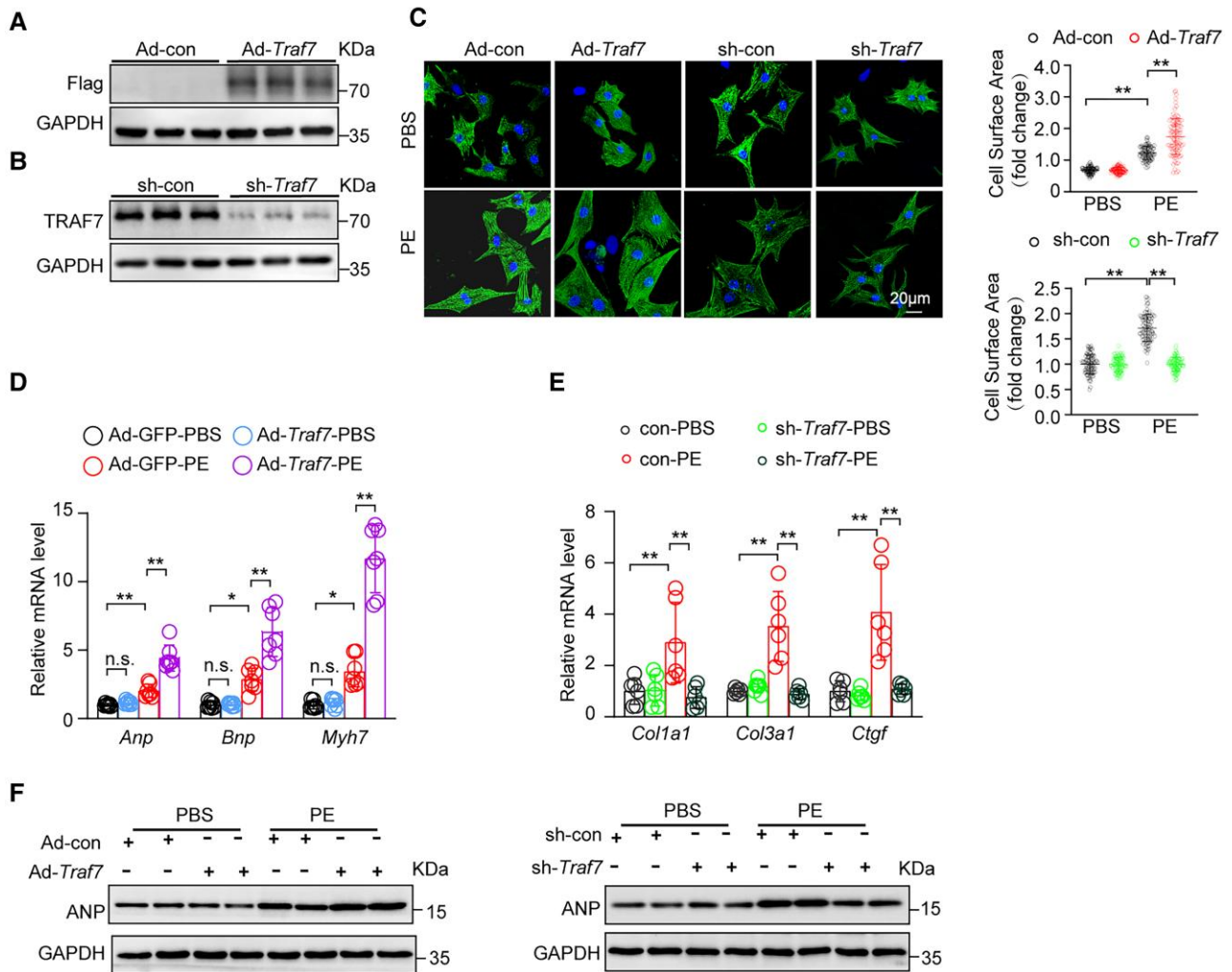
Figure 2 TRAF7 promotes cardiomyocytes hypertrophy *in vitro*. (*A*) Western blot analysis of TRAF7 protein expression in NRCMs infected with adenovirus Traf7 (Ad- *Traf7*) or Ad-con as control (*n* = 6). (*B*) Western blot analysis of TRAF7 protein expression in NRCMs infected with Adsh-*Traf7* or Adsh-con as control (*n* = 6). (*C*) Representative images and quantitative results of immunofluorescence straining of α-actinin (100 cells were counted per group). Scale bar: 20 μm. (*D*) the relative mRNA expression of cardiac hypertrophy-related foetal gene (*Anp, Bnp,* and *Myh7*) in the NRCMs infected with ad-*Traf7* or ad-con as control (*n* = 7). Gene expression was normalized to the mRNA levels of *Gapdh*. (*E*) The relative mRNA expression of cardiac fibrosis-related genes (*Col1a1, Col3a1, and Ctgf*) in the NRCMs infected with Adsh-*Traf7* or Adsh-con as control (*n* = 6). Gene expression was normalized to the mRNA levels of *Gapdh*. (*F*) ANP expression in neonatal rat cardiomyocytes (NRCMs) overexpress or down express TRAF7 treated with PE (50 μM) 24 h compared with corresponding control (*n* = 5). All data are shown as the mean ± SD. Significance analysed by one-way ANOVA with the Bonferroni analysis for data meeting homogeneity or Tamhane's T2 post hoc analysis. *$P < 0.05$, **$P < 0.01$.

phenotype showed that the DEGs were significantly associated with the following biological processes: positive regulation of RAS protein signal transduction, N-terminal protein amino acid modification, intracellular protein transmembrane transport, fibre development, heart contraction, heart rate, the force of heart contraction, and cardiac muscle hypertrophy (*Figure 5C*). Gene heatmaps for cardiac phenotypes are shown in *Figure 5D* and *E*.

To explore the underlying mechanisms by which Traf7 influences pathological cardiac hypertrophy, we performed a Kyoto Encyclopedia of Genes and Genomes (KEGG) pathway enrichment analysis based on RNA-seq datasets from PE-induced NRCMs infected with control or *Traf7* adenovirus. The data showed that MAPK signalling was the most significantly enriched pathway after TRAF7 overexpression (*Figure 5F*).

We subsequently conducted experiments to determine whether TRAF7 had any effect on the activation of MAPK-related proteins. The

results indicated that through *in vitro* overexpression of TRAF7, there was a notable activation in ASK1, JNK, and p38 phosphorylation in PE-induced NRCMs, whereas the p-ERK1/2 level remained unaffected by TRAF7 overexpression (*Figure 5G*). In parallel, *in vivo* experiments demonstrated that the phosphorylation levels of ASK1, JNK, and P38 were significantly increased in TAC-induced TRAF7-overexpressing mice compared with the control group. Furthermore, TRAF7 overexpression did not affect ERK1/2 (*Figure 5I*). Conversely, TRAF7 down-regulation in NRCMs reduced the activation of ASK1, JNK and P38 after PE administration and in heart tissues of *Traf7*-CKO mice detected a lower level of activation of ASK1, JNK, P38, but not ERK compared with the control group 4 weeks after TAC (*Figure 5H* and *J*). All WB strips of *Figure 5F–J* are quantified in Supplementary material online, *Figure S5A–D*. These results indicated that TRAF7 could regulate the ASK1-JNK1/2/p38 axis by promoting the phosphorylation of ASK1, as ASK1 can regulate the activation of JNK and P38, but not ERK.
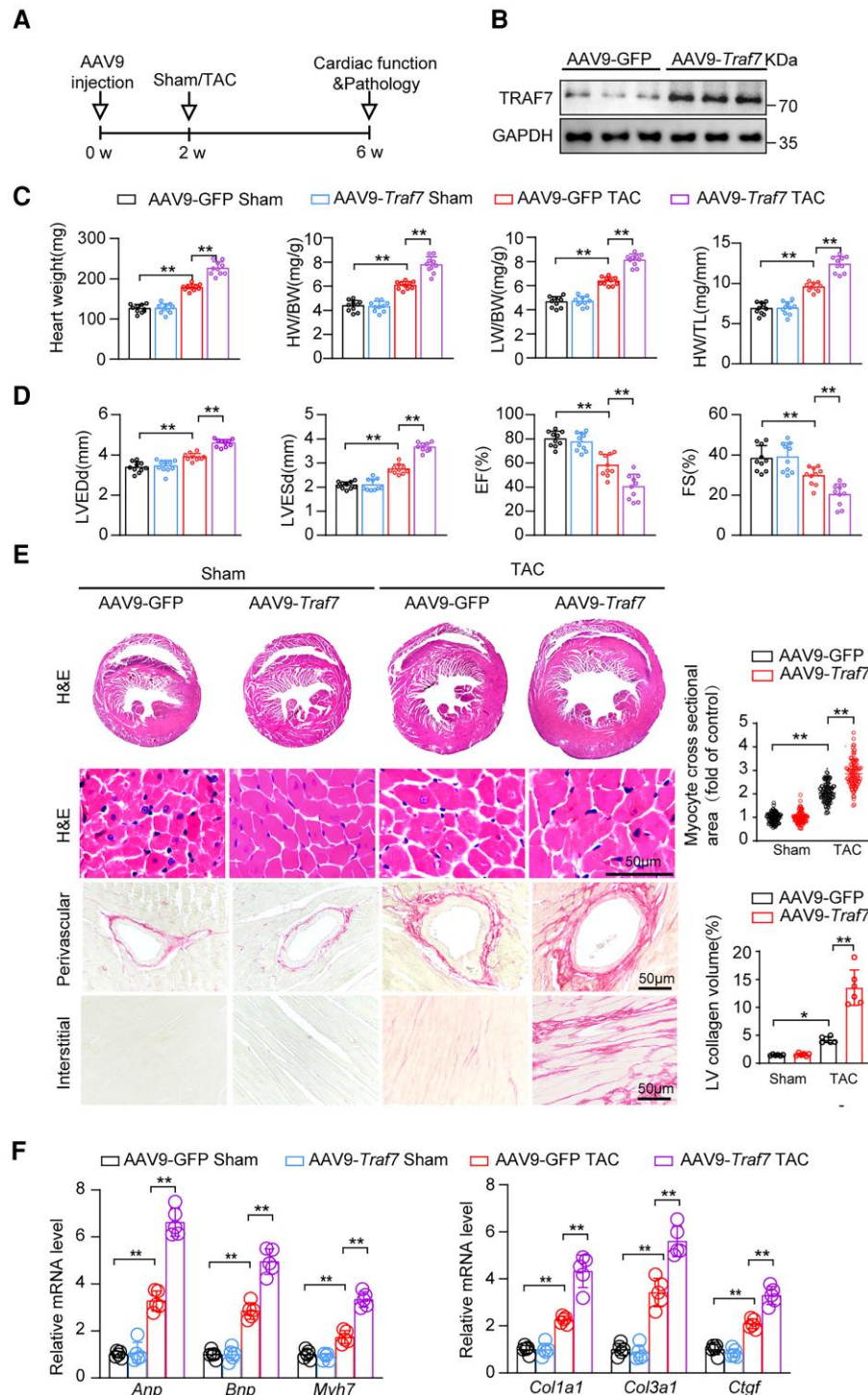
Figure 3 Cardiac-specific overexpression of TRAF7 exacerbates HF progression *in vivo*. (*A*) Schematic outline of the experimental work plan for AAV9-mediated overexpression of TRAF7 in mice. (*B*) Western blots further confirm the up-regulation of TRAF7 in mouse hearts harvested from mice injected with TRAF7 compared with the AAV9-GFP as control (*n* = 5). (*C*) Statistical analysis of heart weight, HW/BW, LW/BW, and HW/TL ratios in AAV9-*Traf7* and AAV9-GFP at 4 weeks after the sham or TAC surgery (*n* = 10 in each group). (*D*) Cardiac function of mice with overexpression of TRAF7 compared with AAV9-GFP, including LVEDd, LVESd, FS, and EF (*n* = 10 in each group). (*E*) Representative images of HE staining and PSR staining in the ventricular sections from AAV9-GFP- or AAV9-*Traf7*-treated mice following sham or TAC (*n* = 6). The quantification of the average CSA and statistical results of the left ventricular interstitial collagen volume are shown in the right of these images. The quantification of the average CSA was analysed by counting100 cells in per group. Scale bar: 50 μm. (*F*) The relative mRNA expression of hypertrophic genes (*Anp, Bnp*, and *Myh7*) (left) and cardiac fibrosis-related genes (*Col1a1, Col3a1, and Ctgf*) (right) in the heart tissues from the indicated mice (*n* = 5). Gene expression was normalized to the mRNA levels of *Gapdh*. Significance analysed by one-way ANOVA with the Bonferroni analysis for data meeting homogeneity or Tamhane's T2 post hoc analysis. *P < 0.05, **P < 0.01. All data are shown as the mean ± SD.
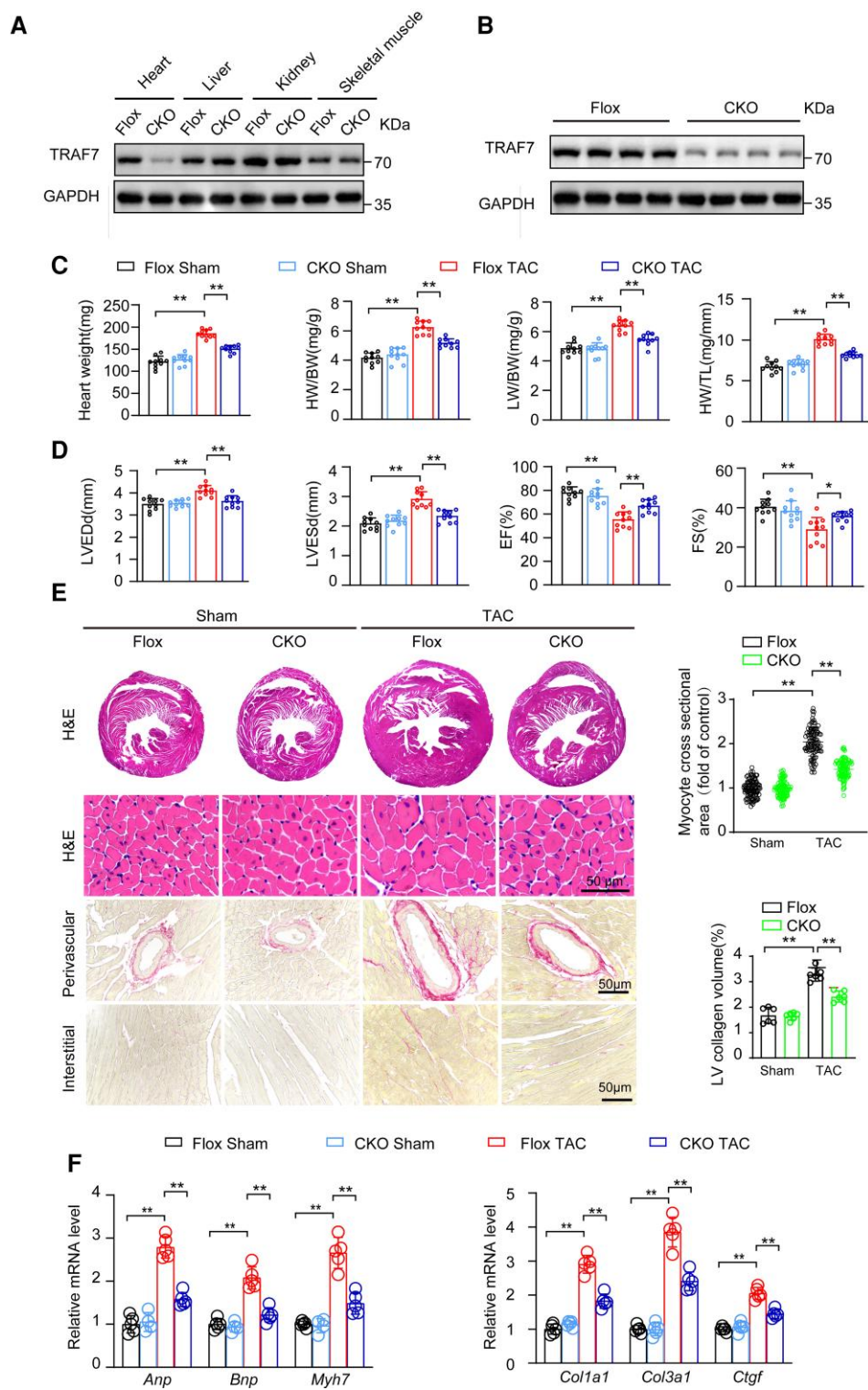
Figure 4 Cardiac-specific *Traf7* knockout (*Traf7*-CKO) inhibits TAC-induced cardiac hypertrophy *in vivo*. (*A*) Western blots of TRAF7 expression in different tissues (*n* = 5). (*B*) Western blots of TRAF7 expression in heart (*n* = 5). (*C*) Statistical analysis of heart weight, HW/BW, LW/BW, and HW/TL ratios in Flox and *Traf7*-CKO mice at 4 w after sham or TAC surgery (*n* = 10). (*D*) Cardiac function comparison between Flox and *Traf7*-CKO mice, including LVEDd, LVESd, FS, and EF (*n* = 10). (*E*) Representative images of HE staining and PSR staining in the ventricular sections from Flox and *Traf7*-CKO mice following sham or TAC (*n* = 6). The quantification of the average CSA and statistical results of the left ventricular interstitial collagen volume are shown in the right of these images. The quantification of the average CSA was analysed by counting 100 cells in per group. Scale bar: 50 μm. (*F*) The relative mRNA expression of hypertrophic genes (*Anp, Bnp, and Myh7*) (left) and cardiac fibrosis-related genes (*Col1a1, Col3a1, and Ctgf*) (right) in the heart tissues from the indicated mice (*n* = 5 in each group). Gene expression was normalized to the mRNA levels of *Gapdh*. Significance analysed by one-way ANOVA with the Bonferroni analysis for data meeting homogeneity or Tamhane's T2 post hoc analysis. *$P < 0.05$, **$P < 0.01$. All data are shown as the mean ± SD.
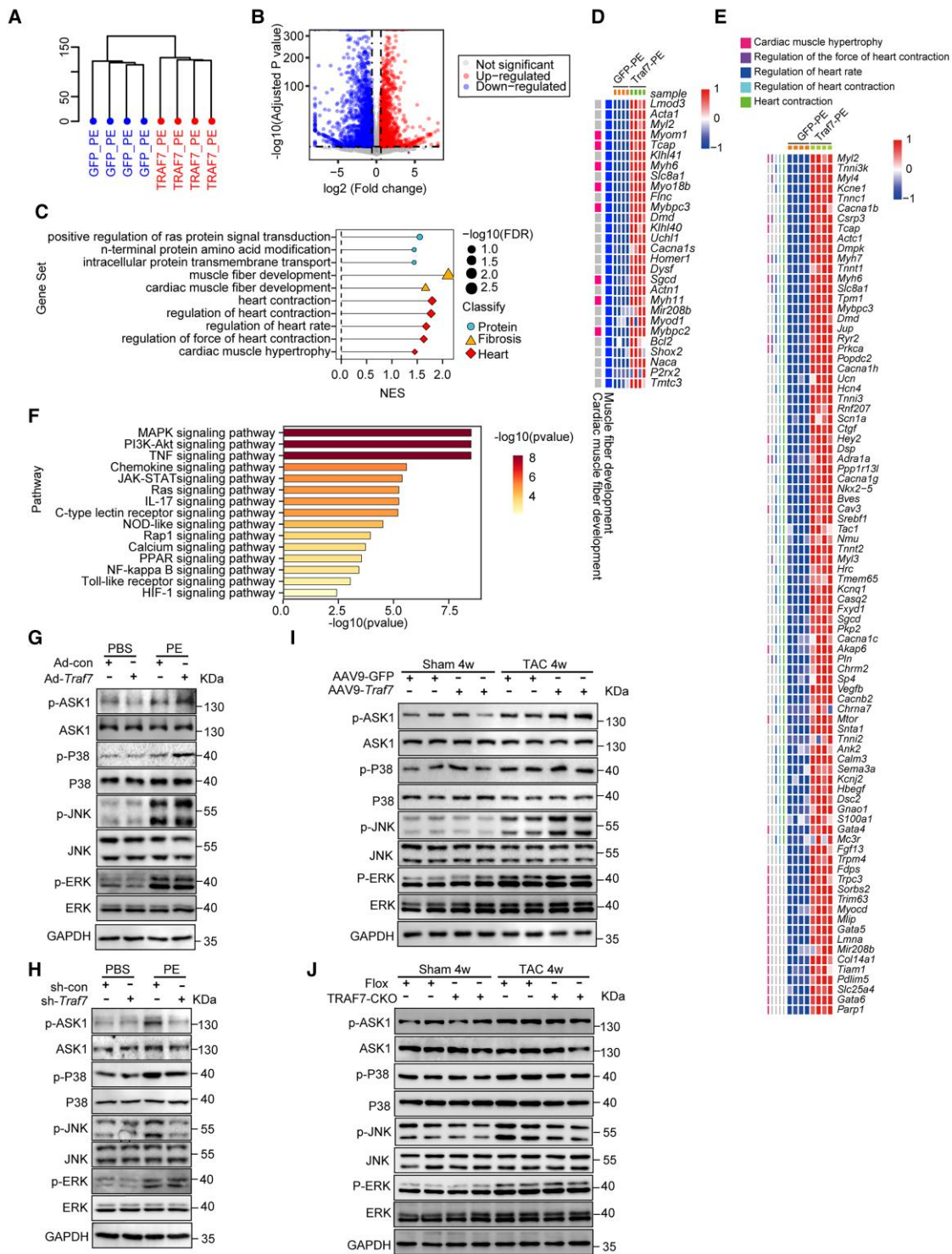
Figure 5 TRAF7 promotes cardiac hypertrophy via MAPK signalling pathway. (*A*) Hierarchical gene cluster analysis of PE-treated NRCMs infected by con or *Traf7* adenovirus (*n* = 4). (*B*) Volcano plot of DEGs (*n* = 4). (*C*) GSEA of cardiac phenotype of biological process (*n* = 4). (*D*) Heatmap showing cardiac phenotypes of muscle fibre development and cardiac muscle fibre development (*n* = 4). (*E*) Heatmap showing cardiac phenotypes of cardiac muscle hypertrophy, regulation of the force of heart contraction, regulation of heart rate, regulation of heart contraction and heart contraction (*n* = 4). (*F*) KEGG pathway enrichment analysis of the identified DEGs based on RNA-seq data set from PE-treated NRCMs infected by GFP or *Traf7* adenovirus (*n* = 4). (*G*) Western blots of total and phosphorylated levels of MAPK signalling-related proteins at 24 h after PBS or PE treatment in NRCMs infected with Ad-*Traf7*. Ad-con used as a control (*n* = 5). (*H*) Western blots of total and phosphorylated levels of MAPK signalling-related proteins at 24 h after PBS or PE treatment in NRCMs infected with Ad-sh*Traf7*. Ad-shRNA was used as a control (*n* = 5). (*I*) Western blots of total and phosphorylated levels of MAPK signalling-related proteins from AAV9-GFP or AAV9-*Traf7*-treated mice at 4 weeks after the sham or TAC surgery (*n* = 5). (*J*) Western blots of total and phosphorylated levels of MAPK signalling-related proteins from Flox or *Traf7*-CKO mice at 4 weeks after the sham or TAC surgery (*n* = 5). Significance analysed by one-way ANOVA with the Bonferroni analysis for data meeting homogeneity or Tamhane's T2 post hoc analysis. *P < 0.05, **P < 0.01. All data are shown as the mean ± SD.
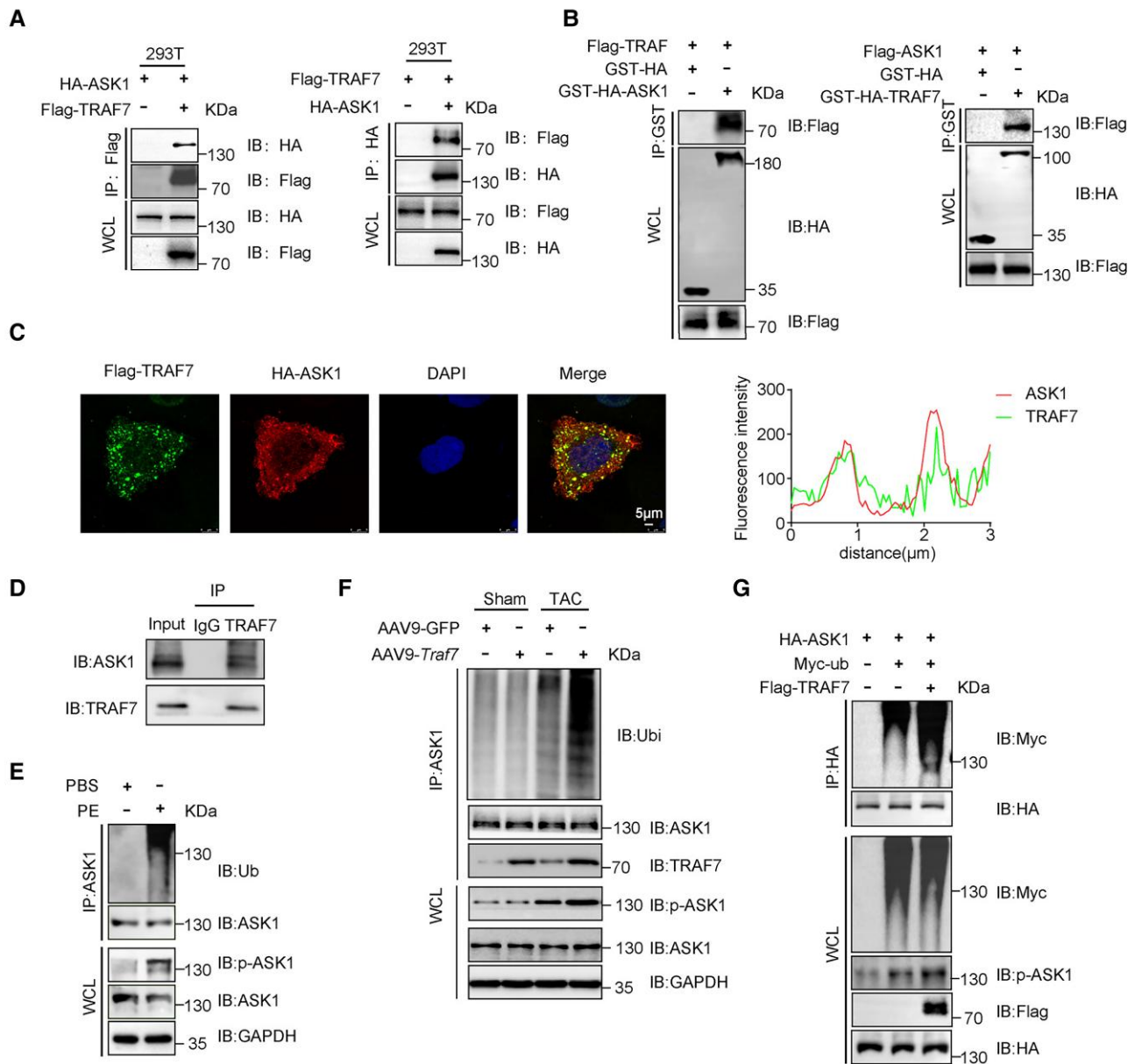
Figure 6 TRAF7 regulates the activation of ASK1 through promoting its ubiquitination. Representative western blots of Co-IP assays in 293T cells transfected with Flag-tagged TRAF7 and HA-tagged ASK1. Flag and HA antibodies were used as western blot probes (*n* = 5). (B) GST precipitation assays showing direct TRAF7–ASK1 binding *in vitro*. GST-HA was used as control (*n* = 5). (C) Representative confocal images of NRCMs co-transfected with Flag-tagged TRAF7 and HA-tagged ASK1. Nuclei were labelled with DAPI (blue). Scale bar: 5 μm (*n* = 5). (D) Representative western blots of Co-IP assays in cardiac tissue. TRAF7 and ASK1 were used as western blot probes. The input group was the positive control, IgG was the negative control. (*n* = 5). (E) Representative western blots of ubiquitinated ASK1 and total ASK1 protein after IP of ASK1 (top) and representative western blots of total ASK1 and p-ASK1 in the WCL of NRCMs treated with PE (50 mM) or PBS for 24 h. Ub, ubiquitin; WCL, whole cell lysate (*n* = 5). (F) Representative western bolt of the ubiquitination and phosphorylation levels of ASK1 in WT and AAV9-*Traf7* mice subjected to sham or TAC surgery. AAV9-GFP sham group was used as control (*n* = 5). (G) Representative western blot of 293T cells transfected with HA-ASK1 and Myc-Ub along with Flag-TRAF7 plasmids which were subjected to immunoprecipitation with anti-HA antibody and tested by HA-tagged, Myc-tagged, HA-tagged, and p-ASK1 antibodies (*n* = 5). Student's two-tailed *t*-test was used to compare the mean values between two groups. Significance analysed by one-way ANOVA with the Bonferroni analysis for data meeting homogeneity or Tamhane's T2 post hoc analysis. *$P < 0.05$, **$P < 0.01$. All data are shown as the mean ± SD.

3.5 TRAF7 regulates the activation of ASK1 by promoting ASK1 ubiquitination

In order to delve deeper into the mechanisms responsible for TRAF's regulation of ASK1, we first examined whether TRAF7 could interact with ASK1. To investigate this question, immunoprecipitation (IP) of TRAF7 and ASK1 was performed, and the results showed that TRAF7 could interact with ASK1 (*Figure 6A*). In addition, the GST pulldown assay further validated the direct interaction between TRAF7 and ASK1 (*Figure 6B*). Moreover, double immunofluorescence staining showed that TRAF7 and
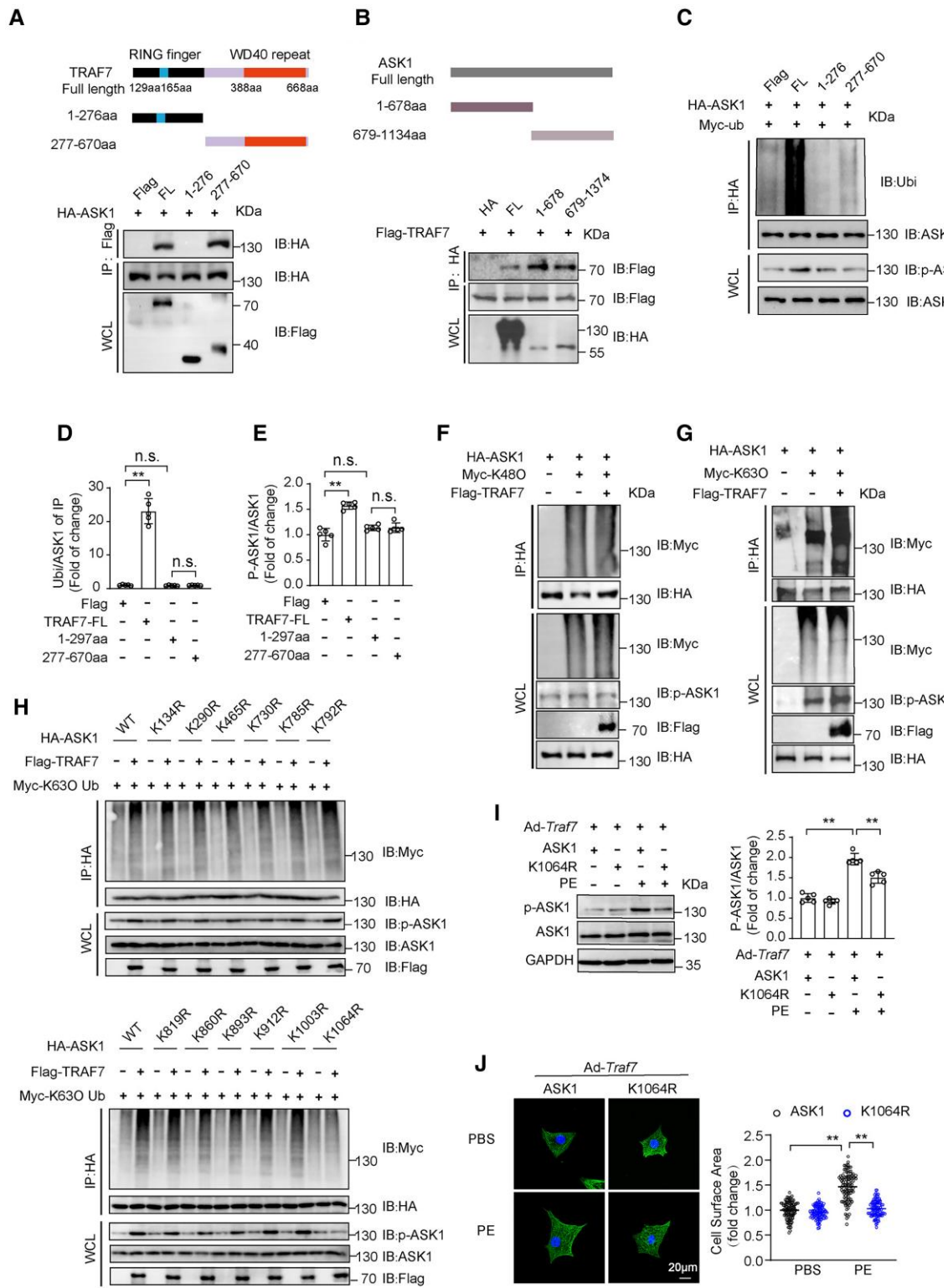
Figure 7 Exploration of the domain, ubiquitination type, and sites of TRAF7-mediated ASK1 ubiquitination. (*A*) Top, schematic of full-length or truncated TRAF7. Bottom, representative western blots with Flag-tagged or HA-tagged antibody after Co-IP of full-length and truncated forms of TRAF7 (*n* = 5). (*B*) Top, schematic of full-length or truncated ASK1. Bottom, representative western blots with Flag-tagged or HA-tagged antibody after Co-IP of full-length and truncated forms of ASK1 (*n* = 5). (*C*) Representative western blot of 293T cells transfected with HA-ASK1 and Myc-Ub along with Flag full-length or truncated TRAF7 plasmids which were subjected to immunoprecipitation with anti-HA antibody and tested by ubiquitin, ASK1, and p-ASK1 antibodies (*n* = 5). (*D*) The quantification of the ubiquitin/ASK1 in (*C*) (*n* = 5). (*E*) The quantification of the p-ASK1/ASK1 in (*C*) (*n* = 5). (*F*) Representative western blot of 293T cells
(continued)

Figure 7 Continued

transfected with HA-ASK1 and Myc-K48O Ub along with or without Flag-TRAF7 plasmids which were subjected to immunoprecipitation with anti-HA antibody and tested by HA-tagged, Myc-tagged, Flag-tagged, and p-ASK1 antibodies ($n = 5$). (G) Representative western blot of 293T cells transfected with HA-ASK1 and Myc-K63O Ub along with or without Flag-TRAF7 plasmids which were subjected to immunoprecipitation with anti-HA antibody and tested by HA-tagged, Myc-tagged, HA-tagged, and p-ASK1 antibodies ($n = 5$). (H) Representative western blot of 293T cells transfected with Flag-TRAF7, Myc-K63O Ub, and HA-ASK1 or ASK1 mutants which were subjected to immunoprecipitation with anti-HA antibody and tested by HA-tagged, Myc-tagged, Flag-tagged, and p-ASK1 antibodies ($n = 5$). (I) Representative western blot of p-ASK1 and ASK1 in neonatal rat cardiomyocytes (NRCMs) infected by Ad-*Traf7* and Ad-*ASK1* or Ad-K1064R and stimulated with PE for 24 h ($n = 5$). (J) Representative images and quantitative results of immunofluorescence straining of α-actinin in NRCMs infected by Ad-*Traf7* and Ad-*ASK1* or Ad-K1064R and stimulated with PE for 24 h (100 cells were counted per group). Scale bar: 20 μm. Significance analysed by one-way ANOVA with the Bonferroni analysis for data meeting homogeneity or Tamhane's T2 post hoc analysis. *$P < 0.05$, **$P < 0.01$. All data are shown as the mean ± SD.

ASK1 were colocalized in NRCMs (*Figure 6C*). We also performed Co-IP using heart tissue of mice, and the results showed that ASK1 and TRAF7 were detected in Input group, indicating the presence of these two proteins. The IgG group in the IP group did not show bands, which ruled out the possibility of non-specific binding, while the anti-TRAF7 group showed bands of both ASK1 and TRAF7, that is, the presence of both proteins in the precipitation complex, indicating the interaction between ASK1 and TRAF7 (*Figure 6C*, see Supplementary material online, *Figure S6F*). As TRAF7 has E3 ubiquitin ligase activity, next we investigated how the ubiquitination of ASK1 changed in response to PE exposure and whether TRAF7 influenced ASK1 activity via its E3 ubiquitin ligase activity. Our findings indicated that PE obviously triggered ASK1 ubiquitination and elevated the level of ASK1 phosphorylation in NRCMs (*Figure 6E*, see Supplementary material online, *Figure S6A*). The ubiquitination and phosphorylation of ASK1 were also examined *in vivo* ubiquitination assay in wild-type (WT) and AAV9-*Traf7* mice subjected to sham or TAC surgery. The results showed that TRAF7 overexpression up-regulated the ubiquitination and phosphorylation of ASK1, which is in parallel with the results in NRCMs (*Figure 6F*, see Supplementary material online, *Figure S6B*). In addition, the increase in ASK1 ubiquitination and phosphorylation was also observed in 293T cells overexpressing TRAF7 (*Figure 6G*, see Supplementary material online, *Figure S6C*). The results indicated that the ASK1 ubiquitination and phosphorylation were related and that TRAF7 could facilitate both processes.

We then explored how TRAF7 affected the ASK1 ubiquitination. IP analysis of ASK1 and the N-terminal and C-terminal regions of TRAF7 showed that the C-terminal region of TRAF7 (277-670 aa) played a crucial role in the interaction between these proteins (*Figure 7A*). In addition, both the C-terminal and the N-terminal regions of ASK1 could bind to TRAF7 (*Figure 7B*). In order to investigate which region of TRAF7 is essential for ASK1 activation, we performed IP analysis of ASK1 and the N-terminal and C-terminal regions of TRAF7, followed by monitoring the ubiquitination and phosphorylation level of ASK1 in 293T cells. The results showed that both the C-terminal region and the N-terminal region of TRAF7 are indispensable for the activation of ASK1 (*Figure 7C–E*).

Then, we analysed the types of ubiquitin modifications on ASK1 that were induced by TRAF7. It has been reported that K48-linked and K63-linked ubiquitination of ASK1 influences the ASK1 activation, and our results showed that K63-linked but not K48-linked ubiquitination of ASK1 was affected by TRAF7 (*Figure 7F* and *G*, see Supplementary material online, *Figure S6D* and *E*).

In order to identify the ubiquitination sites responsible for TRAF7-mediated Lys63-linked ubiquitination of ASK1, a series of ASK1 mutants (K134R, K290R, K465R, K730R, K785R, K792R, K819R, K860R, K893R, K912R, K1003R, K1064R) were constructed according to Bai's report,[20] and the level of K63-linked ubiquitination modification in the presence or absence of TRAF7 was measured by *in vivo* ubiquitination assays. We found that, in comparison with WT ASK1, most of the mutants of ASK1 had no effect on ASK1 activation influenced by TRAF7 except for K1064R (*Figure 7H*). To further confirm the impact of the K1064R mutation on ASK1 in cardiomyocytes, we infected cardiomyocytes with

adenovirus of TRAF7 and ASK1 or K1064R and stimulated cells with PE. It showed that K1064R of ASK1 inhibited the ASK1 phosphorylation activation (*Figure 7I*). The resulting cells were then assessed for hypertrophy using α-actinin staining (*Figure 7J*). These findings showed that K1064R had a significant inhibitory effect for ASK1 phosphorylation and cardiomyocyte hypertrophy in TRAF7 overexpression under PE stimuli.

In summary, the results indicated that overexpressing TRAF7 resulted in an elevated level of K63-linked polyubiquitination of ASK1, and K1064 of ASK1 is the ubiquitination site responsible for TRAF7-mediated Lys63-linked ubiquitination, and consequently triggering ASK1 phosphorylation activation.

3.6 ASK1 is the target by which TRAF7 induces cardiac hypertrophy

To further explore whether TRAF7 regulates cardiac hypertrophy through ASK1 activation, we established rescue experiments *in vitro* by inhibiting ASK1 activation with the ASK1-specific inhibitor GS4997, in the presence of TRAF7 overexpression. The results showed that the CSA of the cell was rescued by GS4997 compared with TRAF7 overexpression after PE stimulation (see Supplementary material online, *Figure S7A*). In addition, the mRNA levels of *Anp*, *Bnp* and *Myh7* were up-regulated by TRAF7 overexpression and reduced by GS4997 treatment upon PE stimulation (see Supplementary material online, *Figure S7B*). Furthermore, TRAF7-induced activation of the ASK1/JNK/p38 axis after PE stimulation was inhibited by GS4997 (see Supplementary material online, *Figure S7C*).

Then, we carried out the rescue experiment using *Ask1*-CKO mice *in vivo*. After proven ASK1 was knocked out in cardiac tissues, we explored the cardiac function, cardiac remodelling, apoptosis level, and signalling pathway influenced by *Ask1*-CKO and TRAF7 overexpression. The results showed that *Ask1*-CKO could remarkably rescue cardiac remodelling induced by pressure overload, while also being capable of suppressing the severe cardiac remodelling induced by TRAF7 overexpression (*Figure 8B–D*). When *Ask1* was cardiac-specific knockout in mice, the signalling pathway of ASK1 and apoptosis level were significantly down-regulated compared with the control group after TAC (see Supplementary material online, *Figure S8A–E*). Although overexpression of TRAF7 led to a higher level of apoptosis after TAC, the *Ask1*-CKO managed to rescue a portion of the heart tissue death, which has a significant difference compared with Flox + AAV9-*Traf7* group (see Supplementary material online, *Figure S8C–E*). It is worth noting that on numerous evaluation dimensions, there was no significant difference observed between *Ask1*-CKO mice with or without AAV9-*Traf7* injection 4 weeks after TAC, which indicated that ASK1 is the crucial downstream target of TRAF7 during TAC-induced cardiac hypertrophy.

4. Discussion

Previous studies have confirmed that TRAF7 is closely related to the activation of MAPKs, especially JNK and P38MAPK during TNF-α signalling in
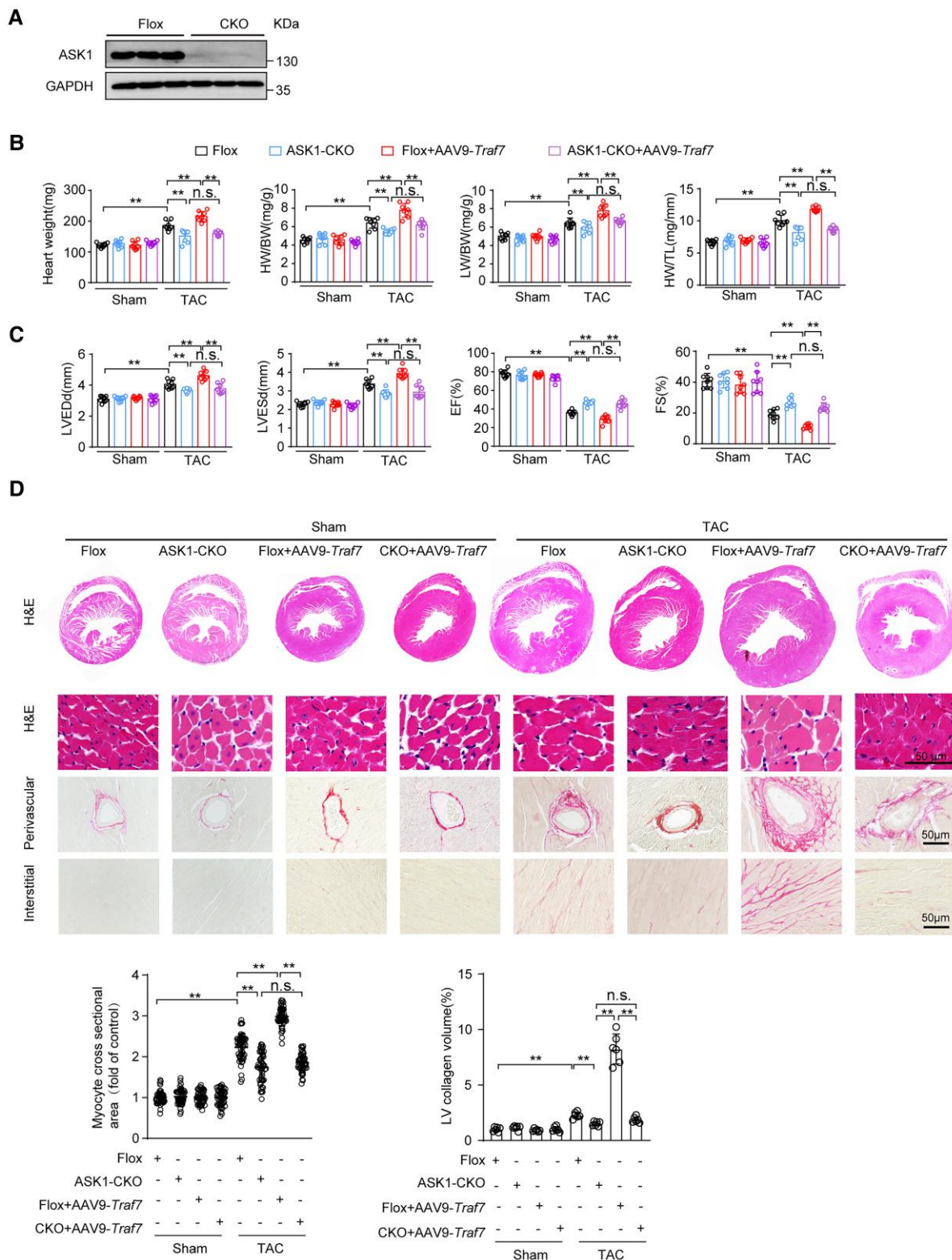
Figure 8 *Ask1*-CKO inhibited TRAF7 overexpression-induced serious cardiac hypertrophy *in vivo*. (*A*) Western blots of ASK1 expression in heart. (*B*) Statistical analysis of heart weight, HW/BW, LW/BW, and HW/TL ratios in Flox and *Ask1*-CKO mice at 4 weeks after sham or TAC surgery injected with or without AAV9-*Traf7* (*n* = 8). (*C*) Cardiac function comparison between Flox and *Ask1*-CKO after sham or TAC surgery injected with or without AAV9-*Traf7*, including LVEDd, LVESd, FS, and EF (*n* = 8). (*D*) Representative images of HE staining and PSR staining in the ventricular sections from Flox and *Ask1*-CKO mice following sham or TAC injected with or without AAV9-*Traf7* (*n* = 6). The quantification of the average CSA and statistical results of the left ventricular interstitial collagen volume are shown below these images. Significance analysed by one-way ANOVA with the Bonferroni analysis for data meeting homogeneity or Tamhane's T2 post hoc analysis. **P* < 0.05, ***P* < 0.01. All data are shown as the mean ± SD.

tumour cells, but the evidence showed that this is due to the activation of MKK3.[12] In this study, we revealed a novel mechanism by which TRAF7 promoted cardiac hypertrophy induced by pressure overload by regulating the important MAPK factor ASK1. Remarkably, overexpressing TRAF7 resulted in an elevated level of K63-linked polyubiquitination of ASK1, and K1064 of ASK1 is the ubiquitination site responsible for TRAF7-mediated Lys63-linked ubiquitination, and consequently triggering ASK1 phosphorylation activation during cardiac hypertrophy. In addition, the application of the ASK1 inhibitor GS4997 and *Ask1*-CKO effectively reversed cardiac hypertrophy induced by TRAF7 overexpression. Therefore, it is reasonable to conclude that TRAF7 is an important factor in regulating cardiac hypertrophy by activating ASK1.

Several studies have confirmed that patients with TRAF7 mutations have varying degrees of congenital heart defects, suggesting that TRAF7 may be related to heart disease.[14,15] However, we did not observe these malformations in *Traf7*-CKO mice during our research. We conjectured that even in the absence of *Traf7*, the occurrence of heart malformations is a probability event. In this study, we measured the expression of TRAF7 in cardiomyocytes and fibroblasts, and TRAF7 protein expression in cardiomyocytes was positively correlated with cardiac hypertrophy. Up-regulation and knockdown of TRAF7 *in vitro* or *in vivo* showed that TRAF7 played an important role in pressure overload–induced cardiac hypertrophy. Further RNA-seq analysis indicated that the overexpression of TRAF7 led to increased expression of genes involved in cardiac muscle fibre development and cardiac muscle hypertrophy. Remarkably, although we did not observe changes in TRAF7 in fibroblasts under hypertrophic stimulation *in vitro*, cardiac fibrosis in TRAF7-overexpressing mice was significantly increased. Besides, cardiac fibrosis in *Traf7*-CKO mice was significantly decreased. Then, we tested the apoptosis level in heart tissues, which is a very important factor influencing cardiac fibrosis.[21] The results showed that TRAF7 overexpression aggravated TAC-induced apoptosis in heart tissues, while *Traf7*-CKO significantly improved the degree of cardiomyocyte apoptosis. In addition, we found that TRAF7-induced cardiac hypertrophy was related to the activation of JNK and P38 MAPK through the regulation of ASK1.

ROS is an important factor in the stress overload and G-protein-coupled receptor agonist (PE/AngII)-induced cardiac remodelling signalling pathway.[22] In *in vitro* studies, we found that TRAF7 can be activated by ROS, and scavenging ROS can inhibit TRAF7 expression caused by G-protein-coupled receptor agonist. Although the specific mechanism is not clear yet, it also helps us understand how TRAF7 is activated.

ASK1, a MAP3K, has been shown to promote pressure overload–induced cardiac hypertrophy and fibrosis.[23] The activation of ASK1 is regulated by oxidative stress, TNF-α, hypertrophic stimulation, and other factors, and ASK1 is typically activated by autophosphorylation.[24,25] Subsequently, Thr838-phosphorylated ASK1 further phosphorylates P38 and JNK.[26,27] It has been proven that the phosphorylation of ASK1 can be mediated by ubiquitinating.[20,28] ASK1 has a C-terminal coiled-coil domain and an N-terminal coiled-coil (NCC) domain. Protein modification at the N terminus determines ASK1 activation or inhibition of ASK1.[29] Except for TRAF1, all other TRAFs have the ring domain with E3 ubiquitin ligase activity, which is necessary for the activation of downstream pathways. TRAF2 could bind to the ASK1 through TRAF domain and applied ring domain to promote the phosphorylation of ASK1.[30] In our study, although TRAF7 lacks the TRAF domain, it still promoted the phosphorylation of ASK1. Our further studies showed that ASK1 could bind to the C-terminal region of TRAF7 (277–670 aa) and lead to endogenous ubiquitination. Then, we examined which ubiquitin ligase mediates the polyubiquitination of ASK1 in the presence of TRAF7. It is currently known that K48 and K63 are related to the ubiquitination of ASK1. WD40 repeats domain is a highly conserved protein and is reported as protein interaction scaffolds containing several β-propeller domains.[31] Up to now, WD40 repeats have not been found to have catalytic activity.[32] In our study, it is WD40 repeats that combined TRAF7 and ASK1 together and ring domains participate in the ubiquitination modification of ASK1. Both N terminus and C terminus are essential for phosphorylation of ASK1 through ubiquitination modification. Different types of ubiquitination lead to different cellular outcomes, and K48-mediated polyubiquitination leads to the hydrolysis of proteins by the proteasome system, which is considered the classic ubiquitination mode. Unlike the ubiquitin chain of at K48, the polyubiquitin chain of K63 does not target a substrate for degradation but influences signalling transport. This effect may be beneficial to the combination of various receptor proteins, especially multidomain adaptor proteins, which allows these proteins to recruit signalling molecules to facilitate downstream signalling pathways.[33] Previous studies have shown that K63-linked polyubiquitination promotes ASK1 activation by causing conformational changes in the NCC domain of ASK1 or by recruiting signalling factors.[34,35] Our study showed that TRAF7 promoted the polyubiquitination of ASK1 via the K63 ubiquitin chain, indicating that TRAF7 may participate in the activation of kinases by mediating ASK1 ubiquitination, thereby promoting downstream signalling. Furthermore, the ubiquitination of lys1064 in ASK1 that TRAF7 mediated is the key to connecting ubiquitination and phosphorylation when facing hypertrophic stimuli.

In addition, to further verify whether TRAF7 regulates cardiac hypertrophy in an ASK1-mediated manner, we treated cells with the ASK1 inhibitor GS4997. GS4997 (also known as selonsertib) has been shown to have antifibrotic and anti-inflammatory effects and has been studied in phase III and II clinical trials for treating non-alcoholic steatohepatitis and diabetic kidney diseases.[12,36] Our results showed that GS4997 inhibited the activation of ASK1 and its downstream JNK/P38MAPK even in the presence of TRAF7 overexpression, which indicated that the negative effects of TRAF7 on the regulation of cardiac hypertrophy could be eliminated by inhibiting the activation of ASK1. *In vivo* rescue experiments using *Ask1*-CKO further illustrate that ASK1 is the downstream target of TRAF7.

There are several limitations in this study, such as how ROS mediates TRAF7 activation. However, we reveal a new mechanism by which TRAF7 regulates the MAPK signalling pathway during the development of cardiac hypertrophy through regulating the activation of ASK1 in an ubiquitination-dependent manner, and this will provide a new strategy for the treatment of cardiac hypertrophy.

Supplementary material

Supplementary material is available at *Cardiovascular Research* online.

Authors' contributions

Q.-Z.T., Y.C., and Y.-T.L. designed the study. Y.C., Y.-T.L., Z.-P.W., Y.-Z.F., H.-X.X., H.-L.Q., and S.-S.W. performed the experiments. Q.-Z.T., Y.C., Y.-T.L., Y.-Z.F., and H.-L.Q. analysed the data. Y.C. and Z.-P.W. drafted the manuscript. Q.-Z.T., Y.Y., H.Z., and M.-L.H. edited the manuscript.

Conflict of interest: The authors have declared that no competing interest exists.

Data availability

The data presented in this manuscript will be made available from the corresponding authors upon reasonable request.

References

1. Shah AM, Cikes M, Prasad N, Li G, Getchevski S, Claggett B, Rizkala A, Lukashevich I, O'Meara E, Ryan JJ, Shah SJ, Mullens W, Zile MR, Lam CSP, McMurray JJV, Solomon SD; PARAGON-HF Investigators. Echocardiographic features of patients with heart failure and preserved left ventricular ejection fraction. *J Am Coll Cardiol* 2019;**74**:2858–2873.

2. Avraham S, Abu-Sharki S, Shofti R, Haas T, Korin B, Kalfon R, Friedman T, Shiran A, Saliba W, Shaked Y, Aronheim A. Early cardiac remodeling promotes tumor growth and metastasis. *Circulation* 2020;**142**:670–683.

3. Wang S-Y, Ni X, Hu K-Q, Meng F-L, Li M, Ma X-L, Meng T-T, Wu H-H, Ge D, Zhao J, Li Y, Su G-H. Cilostazol alleviate nicotine induced cardiomyocytes hypertrophy through modulation of autophagy by CTSB/ROS/p38MAPK/JNK feedback loop. *Int J Biol Sci* 2020;**16**:2001–2013.

4. Meijles DN, Cull JJ, Markou T, Cooper S, Haines Z, Fuller SJ, O'Gara P, Sheppard MN, Harding SE, Sugden PH, Clerk A. Redox regulation of cardiac ASK1 (apoptosis signal-regulating kinase 1) controls p38-MAPK (mitogen-activated protein kinase) and orchestrates cardiac remodeling to hypertension. *Hypertension* 2020;**76**:1208–1218.

5. Li J, Liu N, Tang L, Yan B, Chen X, Zhang J, Peng C. The relationship between TRAF6 and tumors. *Cancer Cell Int* 2020;**20**:429.

6. Divakaran VG, Evans S, Topkara VK, Diwan A, Burchfield J, Gao F, Dong J, Tzeng H-P, Sivasubramanian N, Barger PM, Mann DL. Tumor necrosis factor receptor-associated factor 2 signaling provokes adverse cardiac remodeling in the adult mammalian heart. *Circ Heart Fail* 2013;**6**:535–543.

7. Jiang X, Deng K-Q, Luo Y, Jiang D-S, Gao L, Zhang X-F, Zhang P, Zhao G-N, Zhu X, Li H. Tumor necrosis factor receptor-associated factor 3 is a positive regulator of pathological cardiac hypertrophy. *Hypertension* 2015;**66**:356–367.

8. Ji Y-X, Zhang P, Zhang X-J, Zhao Y-C, Deng K-Q, Jiang X, Wang P-X, Huang Z, Li H. The ubiquitin E3 ligase TRAF6 exacerbates pathological cardiac hypertrophy via TAK1-dependent signaling. *Nat Commun* 2016;**7**:11267.

9. Bian Z, Dai J, Hiroyasu N, Guan H, Yuan Y, Gan L, Zhou H, Zong J, Zhang Y, Li F, Yan L, Shen D, Li H, Tang Q. Disruption of tumor necrosis factor receptor associated factor 5 exacerbates pressure overload cardiac hypertrophy and fibrosis. *J Cell Biochem* 2014;**115**:349–358.

10. He H, Wu Z, Li S, Chen K, Wang D, Zou H, Chen H, Li Y, Liu Z, Qu C. TRAF7 enhances ubiquitin-degradation of KLF4 to promote hepatocellular carcinoma progression. *Cancer Lett* 2020;**469**:380–389.

11. Li D-J, Tong J, Li Y-H, Meng H-B, Ji Q-X, Zhang G-Y, Zhu J-H, Zhang W-J, Zeng F-Y, Huang G, Hua X, Shen F-M, Wang P. Melatonin safeguards against fatty liver by antagonizing TRAFs-mediated ASK1 deubiquitination and stabilization in a beta-arrestin-1 dependent manner. *J Pineal Res* 2019;**67**:e12611.

12. Zotti T, Vito P, Stilo R. The seventh ring: exploring TRAF7 functions. *J Cell Physiol* 2012;**227**:1280–1284.

13. Zotti T, Scudiero I, Vito P, Stilo R. The emerging role of TRAF7 in tumor development. *J Cell Physiol* 2017;**232**:1233–1238.

14. Accogli A, Scala M, Pavanello M, Severino M, Gandolfo C, De Marco P, Musacchia F, Torella A, Pinelli M, Nigro V, Capra V. Sinus pericranii, skull defects, and structural brain anomalies in TRAF7-related disorder. *Birth Defects Res* 2020;**112**:1085–1092.

15. Castilla-Vallmanya L, Selmer KK, Dimartino C, Rabionet R, Blanco-Sanchez B, Yang S, Reijnders M, van Essen AJ, Oufadem M, Vigeland MD, Stadheim B, Houge G, Cox H, Kingston H, Clayton-Smith J, Innis JW, Iascone M, Cereda A, Gabbiadini S, Chung WK, Sanders V, Charrow J, Bryant E, Millichap J, Vitobello A, Thauvin C, Mau-Them FT, Faivre L, Lesca G, Labalme A, Rougeot C, Chatron N, Sanlaville D, Christensen KM, Kirby A, Lewandowski R, Gannaway R, Aly M, Lehman A, Clarke L, Graul-Neumann L, Zweier C, Lessel D, Lozic B, Aukrust I, Peretz R, Stratton R, Smol T, Dieux-Coeslier A, Meira J, Wohler E, Sobreira N, Beaver EM, Heeley J, Briere LC, High FA, Sweetser DA, Walker MA, Keegan CE, Jayakar P, Shinawi M, Kerstjens-Frederikse WS, Earl DL, Siu VM, Reesor E, Yao T, Hegele RA, Vaske OM, Rego S, Shapiro KA, Wong B, Gambello MJ, McDonald M, Karlowicz D, Colombo R, Serretti A, Pais L, O'Donnell-Luria A, Wray A, Sadedin S, Chong B, Tan TY, Christodoulou J, White SM, Slavotinek A, Barbouth D, Morel SD, Parisot M, Bole-Feysot C, Nitschke P, Pingault V, Munnich A, Cho MT, Cormier-Daire V, Balcells S, Lyonnet S, Grinberg D, Amiel J, Urreizti R, Gordon CT. Phenotypic spectrum and transcriptomic profile associated with germline variants in TRAF7. *Genet Med* 2020;**22**:1215–1226.

16. Lin JH, Zhang JJ, Lin S-L, Chertow GM. Design of a phase 2 clinical trial of an ASK1 inhibitor, GS-4997, in patients with diabetic kidney disease. *Nephron* 2015;**129**:29–33.

17. Jungmann A, Leuchs B, Rommelaere J, Katus HA, Muller OJ. Protocol for efficient generation and characterization of adeno-associated viral vectors. *Hum Gene Ther Method* 2017;**28**:235–246.

18. Rangrez AY, Borlepawar A, Schmiedel N, Deshpande A, Remes A, Kumari M, Bernt A, Christen L, Helbig A, Jungmann A, Sossalla S, Tholey A, Muller OJ, Frank D, Frey N. The E3 ubiquitin ligase HectD3 attenuates cardiac hypertrophy and inflammation in mice. *Commun Biol* 2020;**3**:562.

19. Jajesniak P, Wong TS. Rapid construction of recombinant plasmids by QuickStep-Cloning. *Methods Mol Biol* 2017;**1472**:205–214.

20. Bai L, Chen M-M, Chen Z-D, Zhang P, Tian S, Zhang Y, Zhu X-Y, Liu Y, She Z-G, Ji Y-X, Li H. F-box/WD repeat-containing protein 5 mediates the ubiquitination of apoptosis signal-regulating kinase 1 and exacerbates nonalcoholic steatohepatitis in mice. *Hepatology* 2019;**70**:1942–1957.

21. Zhao J, Yin M, Deng H, Jin FQ, Xu S, Lu Y, Mastrangelo MA, Luo H, Jin ZG. Cardiac Gab1 deletion leads to dilated cardiomyopathy associated with mitochondrial damage and cardiomyocyte apoptosis. *Cell Death Differ* 2016;**23**:695–706.

22. Hirotani S, Otsu K, Nishida K, Higuchi Y, Morita T, Nakayama H, Yamaguchi O, Mano T, Matsumura Y, Ueno H, Tada M, Hori M. Involvement of nuclear factor-κB and apoptosis signal-regulating kinase 1 in G-protein-coupled receptor agonist-induced cardiomyocyte hypertrophy. *Circulation* 2002;**105**:509–515.

23. Jiang L, Ren L, Guo X, Zhao J, Zhang H, Chen S, Le S, Liu H, Ye P, Chen M, Xia J. Dual-specificity phosphatase 9 protects against cardiac hypertrophy by targeting ASK1. *Int J Biol Sci* 2021;**17**:2193–2204.

24. Zhong P, Yuan M, Kong B, Huang H. ASK-1, a new target in treating cardiorenal syndrome (CRS). *Int J Cardiol* 2020;**316**:208.

25. Xu W, Zhang L, Zhang Y, Zhang K, Wu Y, Jin D. TRAF1 exacerbates myocardial ischemia reperfusion injury via ASK1-JNK/p38 signaling. *J Am Heart Assoc* 2019;**8**:e12575.

26. Tobiume K, Matsuzawa A, Takahashi T, Nishitoh H, Morita K, Takeda K, Minowa O, Miyazono K, Noda T, Ichijo H. ASK1 is required for sustained activations of JNK/p38 MAP kinases and apoptosis. *EMBO Rep* 2001;**2**:222–228.

27. Mantzaris MD, Bellou S, Skiada V, Kitsati N, Fotsis T, Galaris D. Intracellular labile iron determines H2O2-induced apoptotic signaling via sustained activation of ASK1/JNK-p38 axis. *Free Radic Biol Med* 2016;**97**:454–465.

28. Zhang P, Wang P-X, Zhao L-P, Zhang X, Ji Y-X, Zhang X-J, Fang C, Lu Y-X, Yang X, Gao M-M, Zhang Y, Tian S, Zhu X-Y, Gong J, Ma X-L, Li F, Wang Z, Huang Z, She Z-G, Li H. The deubiquitinating enzyme TNFAIP3 mediates inactivation of hepatic ASK1 and ameliorates nonalcoholic steatohepatitis. *Nat Med* 2018;**24**:84–94.

29. Fujino G, Noguchi T, Matsuzawa A, Yamauchi S, Saitoh M, Takeda K, Ichijo H. Thioredoxin and TRAF family proteins regulate reactive oxygen species-dependent activation of ASK1 through reciprocal modulation of the N-terminal homophilic interaction of ASK1. *Mol Cell Biol* 2007;**27**:8152–8163.

30. Liu H, Nishitoh H, Ichijo H, Kyriakis JM. Activation of apoptosis signal-regulating kinase 1 (ASK1) by tumor necrosis factor receptor-associated factor 2 requires prior dissociation of the ASK1 inhibitor thioredoxin. *Mol Cell Biol* 2000;**20**:2198–2208.

31. Schapira M, Tyers M, Torrent M, Arrowsmith CH. WD40 repeat domain proteins: a novel target class? *Nat Rev Drug Discov* 2017;**16**:773–786.

32. Kim Y, Kim S-H. WD40-repeat proteins in ciliopathies and congenital disorders of endocrine system. *Endocrinol Metab* 2020;**35**:494–506.

33. Laine A, Ronai Z. Ubiquitin chains in the ladder of MAPK signaling. *Sci Stke* 2005;**2005**:e5.

34. Fukuyo Y, Kitamura T, Inoue M, Horikoshi NT, Higashikubo R, Hunt CR, Usheva A, Horikoshi N. Phosphorylation-dependent Lys63-linked polyubiquitination of Daxx is essential for sustained TNF-α-induced ASK1 activation. *Cancer Res* 2009;**69**:7512–7517.

35. Nishitoh H, Saitoh M, Mochida Y, Takeda K, Nakano H, Rothe M, Miyazono K, Ichijo H. ASK1 is essential for JNK/SAPK activation by TRAF2. *Mol Cell* 1998;**2**:389–395.

36. Harrison SA, Wong VW-S, Okanoue T, Bzowej N, Vuppalanchi R, Younes Z, Kohli A, Sarin S, Caldwell SH, Alkhouri N, Shiffman ML, Camargo M, Li G, Kersey K, Jia C, Zhu Y, Djedjos CS, Subramanian GM, Myers RP, Gunn N, Sheikh A, Anstee QM, Romero-Gomez M, Trauner M, Goodman Z, Lawitz EJ, Younossi Z; STELLAR-3; STELLAR-4 Investigators. Selonsertib for patients with bridging fibrosis or compensated cirrhosis due to NASH: results from randomized phase III STELLAR trials. *J Hepatol* 2020;**73**:26–39.